The International Journal of Cardiovascular Imaging
https://doi.org/10.1007/s10554-025-03475-x

REVIEW

Diagnostic accuracy of discovery NM 530c CZT SPECT for myocardial perfusion imaging in coronary artery disease: a systematic review and meta-analysis

Muhammad Arham[1] · Allah Dad[1] · Mohammad Hamza Bin Abdul Malik[2] · Talha Sajjad[1] · Muhammad Awais Bin[1] · Faseeh Haider[3] · Mishal Khan[4] · Anfal Hamza[1] · Muhammad Hammad Arif[5] · Muhammad Ahmad Qureshi[6] · Ali Bin Abdul Jabbar[7] · Muhammad Abdullah Javed[8] · Kinza Bakht[1]

Received: 4 June 2025 / Accepted: 21 July 2025

Abstract

Coronary artery disease (CAD) is the leading cause of cardiovascular mortality (CVD), accounting for 1 in 5 CVD-related deaths. The advent of non-invasive imaging modalities has driven the use of myocardial perfusion imaging (MPI) to enhance diagnostic accuracy and improve clinical outcomes in CAD. Building on the role of myocardial perfusion imaging (MPI), this meta-analysis assesses the diagnostic accuracy of the Discovery NM 530c CZT SPECT for CAD compared with invasive coronary angiography (ICA±FFR) and noninvasive modalities, including PET, MRI, and coronary CT angiography. A systematic search of six databases was conducted to identify studies evaluating the diagnostic accuracy of the NM 530c CZT-SPECT for detecting CAD. Comparator modalities included ICA±FFR, PET, MRI, or coronary CTA performed within 90 days. Diagnostic performance was assessed using pooled sensitivity, specificity, summary receiver operating characteristic (SROC) curves, and diagnostic odds ratio (DOR), using R (v2024.12.0+467) with the "meta" and "mada" packages. A bivariate meta-analysis of 11 studies showed a pooled sensitivity of 83.5% (95% CI: 77.3–88.3%) and specificity of 75.8% (95% CI: 67.8–82.3%), with an AUC of 0.858 and diagnostic odds ratio (DOR) of 15.9. Likelihood ratios were 3.45 (positive) and 0.22 (negative). The SSS≥4 subgroup showed the highest sensitivity (0.881) and DOR (19.21). The univariate random-effects model yielded a pooled sensitivity of 83% and specificity of 77%. Heterogeneity was moderate, and Deeks' test showed no publication bias ($p=0.83$). This meta-analysis establishes the Discovery NM 530c CZT SPECT as a reliable and clinically effective non-invasive modality for detecting coronary artery disease (CAD), with a pooled sensitivity of 0.835, specificity of 0.758, and AUC of 0.858, supporting its diagnostic utility across diverse clinical settings.

Keywords Coronary Artery Disease · Single Photon Emission Computed Tomography Computed Tomography · Myocardial Perfusion Imaging

Introduction

Myocardial Perfusion Imaging (MPI) is a non-invasive diagnostic procedure used to assess myocardial blood flow and detect areas of ischemia. The technique involves injecting a small dose of radioactive contrast into the bloodstream, which is absorbed by the cardiac myocytes, allowing the identification of regions that may not be adequately perfused [1]. Among various imaging modalities available for MPI, Single Positron Emission Computed Tomography (SPECT) and Positron Emission Tomography (PET) are used most commonly. While PET offers higher accuracy in measuring myocardial blood flow, its application is limited by high costs, reliance on volatile radiotracers, and availability issues [2]. This makes SPECT a preferred option due to its lower operational cost and broader accessibility despite its historically lower sensitivity and relatively longer imaging times [3].

Extended author information available on the last page of the article

Published online: 07 August 2025

Before non-invasive imaging became widely available, Invasive Coronary Angiography (ICA) was the gold standard for detecting CAD. Although ICA allows direct visualization of coronary vessels, it is limited in its ability to assess the functional impact of blockages or detect microvascular disease [4, 5]. Non-invasive methods, such as MPI, offer functional insights into myocardial ischemia without the risks associated with invasive procedures. Fractional Flow Reserve (FFR), frequently used in conjunction with ICA, provides additional functional assessment by evaluating the significance of coronary stenosis [6].

Recent advancements in SPECT technology, including the Discovery NM 530c CZT, which utilizes cadmium-zinc-telluride (CZT) detectors, have overcome some of the limitations of earlier SPECT systems. These advancements enhance sensitivity, facilitate faster imaging, and minimize radiation exposure [7, 8]. However, while the Discovery NM 530c CZT system shows promise, its diagnostic accuracy compared to established standards, such as ICA and PET, remains underexplored. Previous meta-analyses, including the parent study, primarily focused on earlier versions of SPECT and did not include data on the NM 530c [9]. This gap in the literature provides the rationale for our current study, which aims to evaluate the diagnostic accuracy of the Discovery NM 530c CZT SPECT system.

We hypothesize that the Discovery NM 530c CZT SPECT system will demonstrate diagnostic accuracy comparable to or superior to that of ICA and PET, offering a valuable non-invasive tool for diagnosing CAD. This meta-analysis aims to address this evidence gap and support the broader clinical implementation of this evidence. By strengthening the case for non-invasive diagnostic approaches, we aim to enhance patient outcomes and increase access to high-quality care [10, 11].

Methodology

Study design and reporting standards

This meta-analysis followed the PRISMA-DTA (Preferred Reporting Items for Systematic Reviews and Meta-Analyses of Diagnostic Test Accuracy Studies) guidelines [12]. The study protocol was registered with the International Prospective Register of Systematic Reviews (PROSPERO) under the ID CRD420251089623.

Search strategy

A systematic literature search was conducted across six databases, PubMed, Embase, Scopus, Google Scholar, Web of Science, and the Cochrane Library, from inception to January 2025, with no restrictions on language or publication year. The search strategy, including relevant MeSH terms, is detailed in the supplementary material Tables 1–2. The reference lists of all included studies were manually screened (using backward snowballing) to identify additional eligible studies. Citation clustering and mapping using LitMap facilitated the exploration of co-cited networks and the identification of potential studies missed in the initial search.

Eligibility criteria

Studies were eligible for inclusion if they utilized NM 530c CZT-SPECT for myocardial perfusion imaging (MPI) and compared the findings with a reference standard, including invasive coronary angiography (ICA) with or without fractional flow reserve (FFR), PET, MRI, or coronary CT angiography. The imaging had to be performed within 90 days of the reference test and included adult patients (≥18 years) with known or suspected coronary artery disease (CAD). Furthermore, studies required sufficient data to derive true positives (TP), false positives (FP), true negatives (TN), and false negatives (FN). Our eligibility criteria mirror those of a recent meta-analysis in a similar context, ensuring comparability [10]. Studies were excluded if they were non-human trials, reviews, editorials, case reports, had a sample size of less than ten, or lacked full-text availability. Additional exclusions included patients with acute myocardial infarction, unstable angina, non-ischemic cardiomyopathy, significant valvular disease, recent revascularization within 90 days, poor-quality imaging, or substantial changes in medication between imaging modalities.

Risk of bias assessment

Two reviewers (AD and FH) independently assessed the risk of bias for each included study. Risk of bias was assessed using the QUADAS-2 tool (Quality Assessment of Diagnostic Accuracy Studies–2). Discrepancies between reviewers were resolved through discussion or, if necessary, adjudicated by a third reviewer (MA).

Data extraction

Extracted variables included information such as the author, year, country, design, sample size, eligibility criteria, full-text availability, and assessed risk of bias. Patient demographic information included age, sex, body mass index (BMI), and comorbidities, including diabetes, hypertension, dyslipidemia, smoking status, and family history of CAD. Imaging protocol details encompassed the type of stress protocol used, injection specifics, radiation dose, and key

CZT imaging parameters such as myocardial blood flow (MBF) and myocardial flow reserve (MFR) cut-off values. Diagnostic performance data were extracted, including TP, TN, FP, FN, sensitivity (SN), specificity(SP), and diagnostic metrics. For studies reporting multiple thresholds, only one was included to preserve statistical independence. The primary endpoint was selected when available; otherwise, the threshold with the highest diagnostic performance was used.

Meta-Analysis

All statistical analyses were performed using R (Version 2024.12.0+467) with relevant packages, including "mada," "meta," "metafor," "mvmeta," and additional visualization libraries. Diagnostic accuracy was analyzed using a bivariate random-effects model to jointly estimate sensitivity and specificity, preserving the two-dimensional structure of test accuracy data [13]. Summary receiver operating characteristic (sROC) curves with 95% confidence intervals were generated. A univariate meta-analysis was constructed to facilitate visualization through forest plots, leave-one-out sensitivity analysis, and subgroup analyses. Diagnostic proportions, including SN and SP, were logit-transformed to satisfy statistical model assumptions [14, 15]. The study employed a DerSimonian-Laird random-effects model with Clopper-Pearson confidence intervals, and τ^2 was estimated according to the guidelines in the Cochrane Handbook [16]. Subgroup analyses were performed based on comparator type (invasive vs. non-invasive), myocardial flow reserve (MFR) cut-offs (standard$\leq$2.0 vs. non-standard), and summed stress scores (SSS) (standard$\geq$4 vs. non-standard). This subgrouping aimed to provide more interpretable and clinically meaningful accuracy estimates [17, 18].

Bivariate heterogeneity testing and publication bias

Between-study heterogeneity was evaluated using both Bayesian and frequentist bivariate models. The Bayesian framework estimated I^2 for sensitivity, specificity, and the joint bivariate model, with 95% credible intervals. In the standard bivariate approach, heterogeneity was assessed by examining the variances of logit-transformed sensitivity and specificity, as well as the area of the joint confidence ellipse in ROC space [19–21]. Publication bias was evaluated using Deeks' funnel plot asymmetry test, regressing log diagnostic odds ratios (log DOR) against the inverse square root of the effective sample size [22]. A p-value$<$0.10 was considered indicative of significant small-study effects.

Results

Study characteristics

A total of 1222 records were identified through systematic database searches, comprising 118 records from PubMed, 210 records from EMBASE, 150 records from Scopus, 118 records from Cochrane CENTRAL, 616 records from Science Direct, and 10 records from ClinicalTrials.com. After removing 425 duplicates, 910 records were screened, of which 747 were excluded. Following full-text assessment, 163 reports were reviewed for eligibility, with 152 excluded due to unmet inclusion criteria (n=147), insufficient data quality (n=4), and overlapping datasets (n=1). Ultimately, eleven studies were included in this meta-analysis (Fig. 1).

The eleven studies included in this meta-analysis were all prospective cohort designs, enrolling 716 adult patients (18 years or older) with known or suspected coronary artery disease (CAD). Studies spanned multiple regions, including Asia and Europe. They evaluated patients with varying cardiovascular risk profiles, with a pooled mean age ranging from 60 to 75 years and a body mass index (BMI) of 24 to 28 kg/m^2. The majority of participants were male, reflecting the typical demographics of CAD. Across studies, the Discovery NM 530c CZT SPECT was used for myocardial perfusion imaging (MPI) and compared with reference standards, including invasive coronary angiography (ICA$\pm$fractional flow reserve, FFR), PET, or other non-invasive modalities. CAD severity was assessed using vessel-level characterization (1–3 vessel disease), MFR, and perfusion metrics, including total perfusion deficit (TPD) and SSS. The quality assessment of the included studies, based on the QUADAS-2 tool, indicated a low risk of bias for each study (Supplementary File Fig. 1), supporting the reliability of the findings. Baseline Study and Patient Characteristics are presented in Table 1.

Table 2 presents a comprehensive summary of stress protocols and myocardial flow parameters from various studies evaluating the diagnostic performance of CZT SPECT for myocardial perfusion imaging in coronary artery disease. It highlights methodological variability across studies in tracer dosage, stress agents, imaging protocols, and comparative modalities such as PET and coronary angiography. Notably, cut-off values for myocardial flow reserve (MFR) and myocardial blood flow (MBF) differ across centers, reflecting heterogeneity in defining functionally significant coronary artery disease. The inclusion of diverse stress agents (e.g., adenosine, regadenoson, ATP) and quantitative tools underscores the complex landscape of standardization in dynamic SPECT imaging.

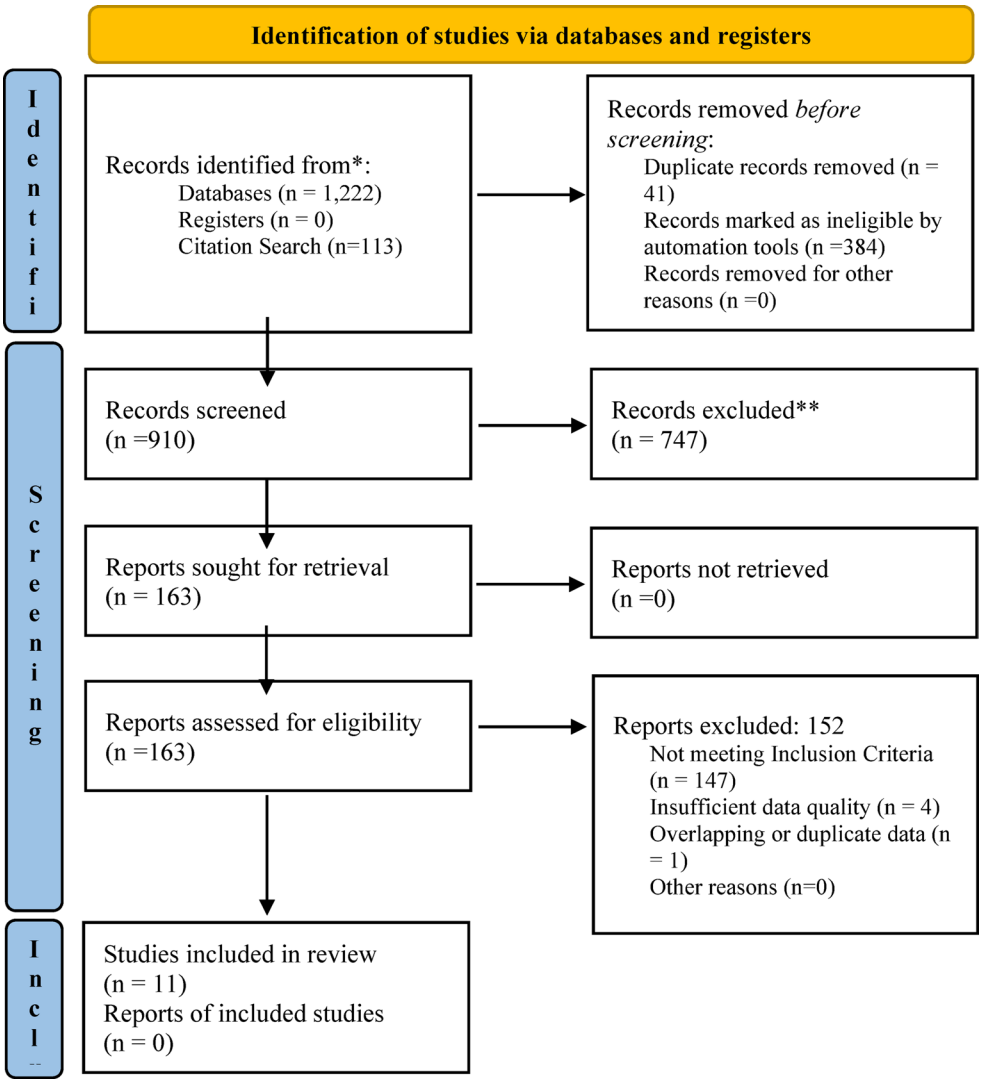

Fig. 1 PRISMA flow diagram of study selection, detailing the identification, screening, eligibility assessment, and inclusion of studies

Bivariate analysis

The bivariate meta-analysis of 11 studies showed a pooled sensitivity of 83.5% (95% CI: 77.3–88.3%) and specificity of 75.8% (95% CI: 67.8–82.3%). The pooled diagnostic odds ratio (DOR) was 15.9 (95% CI: 7.8–24.0). The positive likelihood ratio (LR+) was 3.45 (95% CI: 2.43–4.48), and the negative likelihood ratio (LR–) was 0.22 (95% CI: 0.15–0.29). Heterogeneity was assessed using both standard and Bayesian bivariate models. In the standard model, the between-study variance was 0.168 for logit-transformed sensitivity and 0.128 for logit-transformed specificity, with the area of the joint confidence ellipse estimated at 0.123. In the Bayesian framework, estimated I^2 values were 46% (95% CrI: 33–60%) for sensitivity, 56% (95% CrI: 44–68%) for specificity, and 45% (95% CrI: 36–54%) for the bivariate model. The bivariate model yielded an AUC of 0.858. The SROC curve is shown in the Supplementary Fig. 2. Diagnostic Test Performance Metrics for individual studies are presented in Table 3..

Among all subgroups, the Standard Summed Stress Score (SSS) group demonstrated the highest sensitivity (0.881) and lowest negative likelihood ratio (0.165), indicating superior diagnostic performance. This subgroup also showed the highest diagnostic odds ratio (DOR: 19.21), supporting its enhanced accuracy in identifying disease presence. Diagnostic Test Performance Metrics for individual studies are presented in Table 4.

Univariate analysis

The random-effects model yielded a pooled sensitivity of 0.83 [95% CI: 0.75–0.88], with moderate heterogeneity (I^2 = 44.7%). Omitting Rene N et al., 2016 increased the pooled sensitivity slightly to 0.84 [95% CI: 0.79–0.88] and reduced heterogeneity to I^2 = 17.1%. Subgroup analyses based on MFR cut-off, SSS cut-off, and comparator type revealed no

Table 1 Baseline study and patient characteristics

Study	Year	Country	Design	Sample size	Age (years)	M/F	BMI (Kg/m^2)	Eligibility criteria		Standard modifiable risk factors				Coronary Artery Disease (CAD)		
								Inclusion criteria	Exclusion criteria	Diabetes	HTN	Lipidemia	Smoking	Family history of CAD	CAD diagnosed	Type of CAD
Raffaele Giubbini et al.	2021	Italy	Prospective Cohort	54	68	37/17	NR	Patients referred for MPI	Contraindications to imaging or vasodilation	13	40	33	14	NR	24	NR
Yoshiko Nishiyama et al.	2014	Japan	Prospective Cohort	279	69	171/99	24.3	Suspected or known CAD referred for stress/rest SPECT	Acute MI, recent revascularization, valvular disease, asthma	112	187	119	124	48	76	1–3 vessel
Jiao Wang et al.	2021	China	Prospective Cohort	49	62.5	26/23	26.7	Adults 18–79 yrs, with CAG data±3 months	Post-revascularization, significant valve/cardiac/pulmonary disease	6	32	19	14	15	33	1–3 vessel
Shinya Shiraishi et al.	2020	Japan	Prospective Cohort	125	75	72/53	23	Normal MPS and CAG within 90 days	Abnormal MPS, CABG, cardiomyopathies, myocarditis	54	98	83	NR	NR	78	1–3 vessel
Fayçal Ben Boullègue et al.	2015	France	Prospective Cohort	23	66	19/4	26	Multivessel CAD confirmed by angiography	NR	4	7	12	12	2	23	1–3 vessel
Sangwon Han et al.	2018	Korea	Prospective Cohort	34	60	25/9	24.7	Known/suspected CAD undergoing FFR	Recent MI, left main CAD, low EF	9	23	25	15	NR	34	1–3 vessel
Rene Nkoulou et al.	2016	Switzerland	Prospective Cohort	28	64	24/8	28	Referred for MPI, underwent both CZT and PET	Revascularization, unstable medications	9	17	18	4	13	NR	NR
Shinya Shiraishi et al.	2015	Japan	Prospective Cohort	55	74	24/31	24	Suspected CAD with CAG within 30 days	Prior CABG/PCI, cardiomyopathies	22	34	29	NR	11	45	1–3 vessel
Masao Miyagawa	2017	Japan	Prospective Cohort	69	69	46/23	24	Suspected or known CAD consenting to MPI	MI, unstable angina, cardiomyopathies, asthma, valve disease	37	55	38	41	19	60	1–3 vessel
Alessia Gimelli	2012	Sweden	Prospective Cohort	148	63	125/23	39	Obese patients (BMI≥30 kg/m²; weight≥95 kg for men, ≥90 kg for women) with known or suspected CAD referred for stress/rest SPECT.	Patients with acute or recent (<3 months) ST-segment elevation MI	58	89	79	46	70	94	1–3 vessel
Alessia Gimelli	2012	Sweden	Prospective Cohort	137	61	101/36	NR	Patients with known or suspected CAD referred for stress–rest gated SPECT	Patients with acute or recent (<3 months) ST-segment elevation MI or unstable angina.	39	45	32	56	68	113	1–3 vessel

CAD Coronary Artery Disease, *MPI* Myocardial Perfusion Imaging, *MPS* Myocardial Perfusion Scintigraphy, *CAG* Coronary Angiography, *FFR* Fractional Flow Reserve, *LV-MFR* Left Ventricular Myocardial Flow Reserve, *MBF* Myocardial Blood Flow, *CABG* Coronary Artery Bypass Grafting, *PCI* Percutaneous Coronary Intervention, *EF* Ejection Fraction, *SSS* Summed Stress Score, *MPR* Myocardial Perfusion Ratio, MI (Myocardial Infarction)

Table 2 Summary of stress protocol and myocardial flow parameters from included studies

Study	Stress protocol	Mean total effective dose	Rest dose	Stress dose	Stress injection protocol	Index test	Comparator	Time between tests	Analysis software used	CZT MFR Cut-off value (Key)
Raffaele Giubbini et al.	Patients received 10–15 MBq of 99mTc-tetrofosmin 20 min before the stress test, followed by a 5-minute pre-stress scan	NR	370 MBq of 99mTc-Tetrofosmin	185 MBq of 99mTc-Tetrofosmin	Maximal vasodilation was achieved with 400 mg regadenoson IV over 10 s, followed by a 185 MBq dose of 99mTc-Tetrofosmin 40 s later	99mTc-Tetrofosmin-CZT SPECT	N13-NH3 PET/CT	Within 2 weeks	CZT data: Corridor-4DM-Reserve-v2015 (INVIA, Ann Arbor, MI, USA); PET data: 4-DM Corridor (INVIA, Ann Arbor, MI, USA); analysis: SPSS 23.0 (IBM, Chicago, IL, USA) or MedCalc (Ostend, Belgium)	2 (for predicting MFR < 2)
Yoshiko Nishiyama et al.	1-day protocol: no caffeine 24 h prior. Stress SPECT with ATP, contrast injection, images in supine/prone. Rest SPECT 4 h later, 90 min post-contrast	4.86–9.58 mSv	740 MBq	296–370 MBq (99mTc-tetrofosmin or 99mTc-sestamibi)	Pharmacological stress with adenosine triphosphate disodium (ATP) infused at 160 $\mu g \cdot kg^{-1} \cdot min^{-1}$ for 5 min	Combined supine and prone MPSusing a cadmium zinc telluride (CZT) gamma camera.	Invasive coronary angiography (CAG).	4 h	Xeleris Ver. 3.0 for reconstruction; QPS for reorientation and polar plot analysis; statistical analysis with SPS v21 and JMP 9.	NR

Table 2 (continued)

Study	Stress protocol	Mean total effective dose	Rest dose	Stress dose	Stress injection protocol	Index test	Comparator	Time between tests	Analysis software used	CZT MFR Cut-off value (Key)
Jiao Wang at al	1-day: ATP stress (3 min), 99mTc-MIBI (555–888 MBq), gated imaging 40–60 min later. 2-day: Rest/stress doses (370–555 MBq), same protocol.	n/a	185–296 MBq (1-day protocol); 370–555 MBq (2-day protocol)	555–888 MBq (1-day protocol); 370–555 MBq (2-day protocol).	ATP stress peaked at 3 min after starting infusion. 99mTc-MIBI injected as a bolus (completed within 5 s). Data collected continuously for 10 min in list mode.	CZT Dynamic SPECT: Quantified MBF and MFR to diagnose CAD.	Traditional Semi-Quantitative Gated MPI	In 1 day protocol: 4 h, In 2 days protocol: 24 h	Xeleris 3.0: Reconstruction; Myoflow Q 1.02: MBF/MFR; QPS: SSS, SRS, SDS, TID analysis.	Stenosis≥50%: 1.61 Stenosis≥75%: 1.15
Shinya Shiraishi MD et al.	Adenosine (0.12 mg/kg/min × 6 min) used for stress; Tl-201 (50–60 MBq) injected at peak, followed by 40 ml saline flush.	15.5 mSv	50–60 MBq	50–60 MBq	Adenosine 0.120 mg/kg/min	Myocardial Perfusion Reserve (MPR) using CZT-SPECT.	Invasive coronary angiography (CAG).	90 days	AZE VirtualPlace Hayabusa version 6.1	MFR < 2.66
Fayçal Ben Bouallègue et al.	1-day rest–stress MPI with 99mTc-tetrofosmin at rest and peak vasodilator stress.	8.4 mSv	220–280 MBq	645–730 MBq	Dipyridamole 0.75 mg/kg	Myocardial Perfusion Reserve (MPR).	CAGand FFR measurements	4 weeks, with an average of 5 ± 8 days after the MPI	QPS/QGS software	MFR < 2
Sangwon Han et al.	Adenosine (140 µg/kg/min for 6 min) stress; 201Tl (44.4–66.6 MBq) IV at peak, 5 mL saline flush; 11-min dynamic CZT SPECT imaging.	9.13 mSv	222–370 MBq	44–66 MBq	Adenosine (140 mcg/kg/min)	NR	FFR during induced hyperemia.	NR	NR	MFR </= 2.0

Table 2 (continued)

Study	Stress protocol	Mean total effective dose	Rest dose	Stress dose	Stress injection protocol	Index test	Comparator	Time between tests	Analysis software used	CZT MFR Cut-off value (Key)
Rene Nkoulou et al.	adenosine stress (0.14 mg/kg/min over 6 min) for both CZT SPECT and PET imaging, with tracer injections 3 min into infusion—13 N-ammonia (1,053 ± 110 MBq) for PET and 99mTc-tetrofosmin (330 ± 33 MBq) for SPECT. Dynamic acquisitions lasted 19 min for PET and 10 min for SPECT, followed by rest imaging with a 50-minute delay for PET and a higher tracer dose for SPECT. This standardized protocol enabled comparative assessment of myocardial blood flow (MBF) and myocardial flow reserve (MFR) “	n/a	−1000 MBq	330 ± 33 MBq	Adenosine (140 mcg/kg/min)	NR	FFR by 13 N-ammonia PET	NR	NR	MFR < 1.26
Shinya Shiraishi MD et al.	Patients underwent pharmacologic stress with adenosine (0.120 mg kg^{-1} min^{-1} for 6 min) and a half-dose injection of Tl-201 at peak stress. Dynamic imaging was performed for 6 min, with continuous monitoring of symptoms, blood pressure, and ECG.	15.5 mSv	50–60 MBq	50–60 MBq	Adenosine 0.120 mg/kg/min	NR	Invasive coronary angiography (CAG).	NR	NR	MFR < 1.5
Masao Miyagawa	ATP (160 µg/kg/min for 5 min) stress, followed by 99mTc injection; dynamic SPECT used to quantify myocardial flow reserve.	6.34 mSv	3 MBq/kg	9 MBq/kg	Adenosine (160 mcg/kg/min)	NR	FFR by 13 N-ammonia PET	NR	NR	MFR < 1.3

Table 2 (continued)

Study	Stress protocol	Mean total effective dose	Rest dose	Stress dose	Stress injection protocol	Index test	Comparator	Time between tests	Analysis software used	CZT MFR Cut-off value (Key)
Alessia Gimelli	Single-day protocol using 99mTc-tetrofosmin	5.10 mSv	370–444 MBq	185–222 MBq	Patients underwent exercise or dipyridamole stress after withholding antianginals for 48 h, based on ability to reach ≥ 85% max HR	CZT camera (Discovery NM 530c)	Invasive coronary angiography (CAG).	NR	Xeleris II; GE Healthcare	NR
Alessia Gimelli	Single-day protocol using 99mTc-tetrofosmin	5.10 mSv	370–444 MBq	185–222 MBq	Patients underwent exercise or dipyridamole stress after withholding antianginals for 48 h, based on ability to reach ≥ 85% max HR	CZT camera (Discovery NM 530c)	Invasive coronary angiography (CAG).	NR	Xeleris II; GE Healthcare	NR

ATP Adenosine Triphosphate, *MBF* Myocardial Blood Flow, *MFR* Myocardial Flow Reserve, *99mTc* Technetium-99 m, *CZT* Cadmium Zinc Telluride, and *SPECT* Single Photon Emission Computed Tomography. Additionally, MPS refers to Myocardial Perfusion Scan, *FFR* Fractional Flow Reserve, *SPSS* Statistical Package for the Social Sciences, and MedCalc statistical software for analysis. Other abbreviations include *ECG* Electrocardiogram, *CAG* Coronary Angiography, *SRS* Sum of Resting Scores, *SSS* Sum of Stress Scores, *SDS* Sum of Difference Scores, *TID* Transient Ischemic Dilation, *QPS* Quantitative Perfusion SPECT, and *QGS* Quantitative Gated SPECT

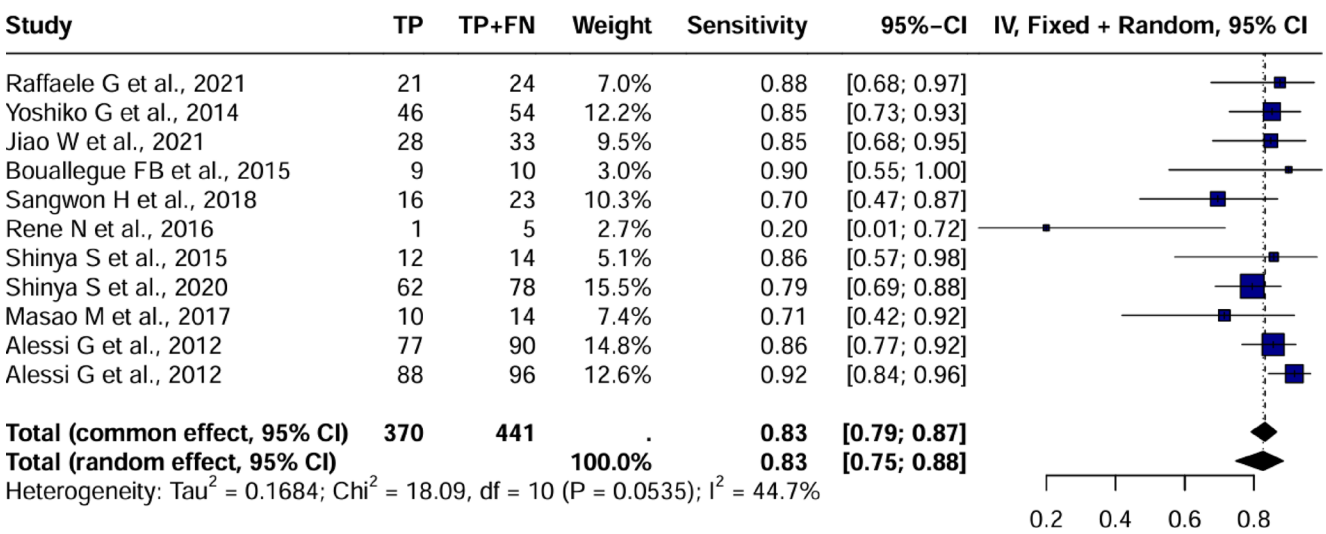

Fig. 2 Forest Plot for Sensitivity

Table 3. Diagnostic test performance metrics for individual studies

Diagnostic Test Performance Metrics for Individual Studies										
Author	TP	FP	TN	FN	TP+FN	FP+TN	TP+FP	TN+FN	SN	SP
Raffaele G et al., 2021	21	10	20	3	24	30	31	23	0.875	0.667
Yoshiko G et al., 2014	46	4	18	8	54	22	50	26	0.852	0.818
Jiao W et al., 2021	28	2	14	5	33	16	30	19	0.848	0.875
Bouallegue FB et al., 2015	9	3	13	1	10	16	12	14	0.9	0.812
Sangwon H et al., 2018	16	8	45	7	23	53	24	52	0.696	0.849
Rene N et al., 2016	1	2	14	4	5	16	3	18	0.2	0.875
Shinya S et al., 2015	12	9	32	2	14	41	21	34	0.857	0.78
Shinya S et al., 2020	62	16	31	16	78	47	78	47	0.795	0.66
Masao M et al., 2017	10	1	13	4	14	14	11	17	0.714	0.929
Alessi G et al., 2012	77	4	4	13	90	8	81	17	0.856	0.5
Alessi G et al., 2012	88	3	6	8	96	9	91	14	0.917	0.667

Abbreviations: TP – True Positive; FP – False Positive; TN – True Negative; FN – False Negative; SP – Specificity; SN – Sensitivity

statistically significant differences. The forest plot is shown in Fig. 2.

The pooled specificity was 0.77 [95% CI: 0.68–0.83], with low-to-moderate heterogeneity (I^2 = 28.9%). After excluding Shinya S et al., 2020, specificity increased slightly to 0.78 [95% CI: 0.70–0.85], and heterogeneity decreased to I^2 = 17.8%. Subgroup analyses based on MFR cut-off, SSS cut-off, and comparator type showed no statistically significant differences. The forest plot is presented in Fig. 3.

Publication bias was assessed using Deeks' funnel plot asymmetry test for the diagnostic odds ratio (DOR). Visual inspection of the Deeks plot revealed no evident asymmetry. The regression analysis showed a non-significant slope ($\beta = -1.605$, $p = 0.83$), indicating no substantial evidence of publication bias (Fig. 4).

Discussion

The findings of the present meta-analysis, based on a bivariate random-effects model of 11 studies, demonstrated a pooled sensitivity of 83.5% (95% CI: 77.3–88.3%) and specificity of 75.8% (95% CI: 67.8–82.3%), with an area under the curve (AUC) of 0.858. The pooled diagnostic odds ratio (DOR) was 15.9 (95% CI: 7.8–24.0), with the highest value observed in the subgroup using an SSS cut-off ≥4 (DOR: 19.21). These results support the diagnostic reliability of the Discovery NM 530c CZT SPECT for evaluating coronary artery disease (CAD).

The area under the curve (AUC) of 0.86 observed for the Discovery NM 530c CZT SPECT system demonstrates competitive diagnostic performance with established modalities. In a comprehensive meta-analysis, the AUCs reported for cardiac magnetic resonance (CMR) and conventional SPECT in patients with suspected or known coronary artery disease (CAD) were 0.92 (95% CI: 0.89–0.94) and 0.87 (95% CI: 0.84–0.90), respectively [23]. Notably, the diagnostic performance of CZT SPECT slightly exceeds that of PET (AUC 0.84 in comparable cohorts), while offering advantages in terms of accessibility and operational cost [24].

In patients with moderate to severe ischemia, SPECT imaging has been associated with improved outcomes following early coronary revascularization [24]. Similarly, the

Table 4 Diagnostic test accuracy metrics based on subgrouping

	Sensitivity	Specificity	Diagnostics odds ratio (DOR)	Likelihood ratio + ve	Likelihood ratio -ve
Comparator Group					
Invasive Comparator Group	0.833 (0.77–0.881)	0.765 (0.679–0.833)	16.202 (7.435–24.97)	3.543 (2.388–4.689)	0.219 (0.146–0.291)
Non Invasive Comparator Group	0.741 (0.365–0.934)	0.797 (0.624–0.903)	11.234 (−4.432-26.9)	3.654 (1.455–5.852)	0.325 (−0.036-0.687)
Summed Stress Score (SSS)					
Standard*	0.881 (0.831–0.918)	0.721 (0.507–0.867)	19.21 (−0.219-39.638)	3.162 (1.047–5.277)	0.165 (0.092–0.238)
Non-Standard	0.822 (0.735–0.885)	0.789 (0.683–0.867)	17.245 (4.267–30.222)	3.895 (2.157–5.633)	0.266 (0.128–0.324)
Myocardial Fractional Reserve (MFR)					
Standard**	0.816 (0.655–0.912)	0.781 (0.655–0.869)	15.772 (2.343–29.202)	3.72 (2.022–5.417)	0.236 (0.082–0.39)
Non-Standard	0.714 (0.536–0.843)	0.801 (0.655–0.895)	10.041 (1.887–18.195)	3.589 (1.628–5.549)	0.357 (0.178–0.537)

*SSS cut-offs: standard defined as ≥4; non-standard other than ≥4

**MFR cut-offs: standard defined as ≤2.0; non-standard other than ≤2.0

2023 ACC/AHA Task Force guidelines support the use of stress PET or SPECT MPI in patients with chronic coronary disease (CCD) who experience persistent changes in symptoms or functional capacity despite guideline-directed medical therapy (GDMT). These imaging strategies are endorsed for detecting the presence and extent of myocardial ischemia, estimating the risk of major adverse cardiovascular events (MACE), and guiding therapeutic decisions [25]. However, it is noteworthy that current guidelines do not yet distinguish between conventional SPECT and advanced CZT-based systems. Emerging data suggest CZT SPECT offers superior per-patient and per-vessel accuracy compared to traditional SPECT/CT, while avoiding additional radiation from CT and maintaining diagnostic integrity despite the absence of attenuation correction [26]. This positions CZT SPECT as a viable, efficient alternative for CAD evaluation. While invasive FFR remains the reference standard, FFRCT achieves AUCs ranging from 0.81 to 0.92 in patients with calcified coronary disease [27–31]. The comparable AUC of CZT SPECT highlights its promise as a pragmatic, non-invasive option in contemporary CAD diagnostics.

The prevalence of CAD is increasing globally, necessitating the development of cutting-edge, non-invasive technologies to improve patient outcomes. MPI is one of these techniques adapted to detect disease, guide therapy, and predict the prognosis [32]. When comparing our findings to those of previous meta-analyses, such as Panjer et al., it was observed that the sensitivity calculated in our study is 1.4% higher than that reported by Panjer et al. [10]. Similarly, the reported DOR of this study is modestly lower than that of a previous meta-analysis. These findings suggest a marginally reduced overall diagnostic performance in our analysis. However, it is worth considering that Panjer's analysis indicated higher heterogeneity and lower sample size (421 in 9 studies and 334 in 6 studies based on NM 530c SPECT), which may have been potential factors that shaped their findings compared to ours. In contrast, the lower heterogeneity observed for sensitivity and specificity in our meta-analysis suggests consistency in diagnostic performance across the included studies.

Another study by Parker et al. included data from 117 studies comprising more than 11,000 patients [33]. Out of these, nearly one-tenth of patients underwent PET imaging, while the others underwent SPECT imaging. The study highlighted that PET had a higher sensitivity of 0.92 and specificity of 0.85 compared to SPECT's sensitivity of 0.88 and specificity of 0.70. Moreover, there was a stark difference in DOR of PET at 48.5 and SPECT at 16.0. However, it is worth mentioning that the findings in the study conducted by Parker et al. are contrary to our observations, as our research also included an assessment of the advanced CZT modality of SPECT, which has higher photon sensitivity and spatial resolution than traditional SPECT [34]. This modality had not been developed when the studies above were conducted. Therefore, technological advancements account for the improved diagnostic accuracy observed in our study.

PET techniques use radiotracers with a high cost burden, significantly hindering their widespread adoption. According to the SPARC study, the two-year costs were highest for PET, at $6,647 per patient, compared to $3,965 for SPECT. After multivariable adjustment, PET costs were 22% significantly higher than those of SPECT [35]. Additionally, most radioisotopes utilized in PET have short half-lives and require in-house cyclotron production, thus limiting the availability of PET. Here lies the main advantage of SPECT. The radiotracers used for SPECT imaging are less

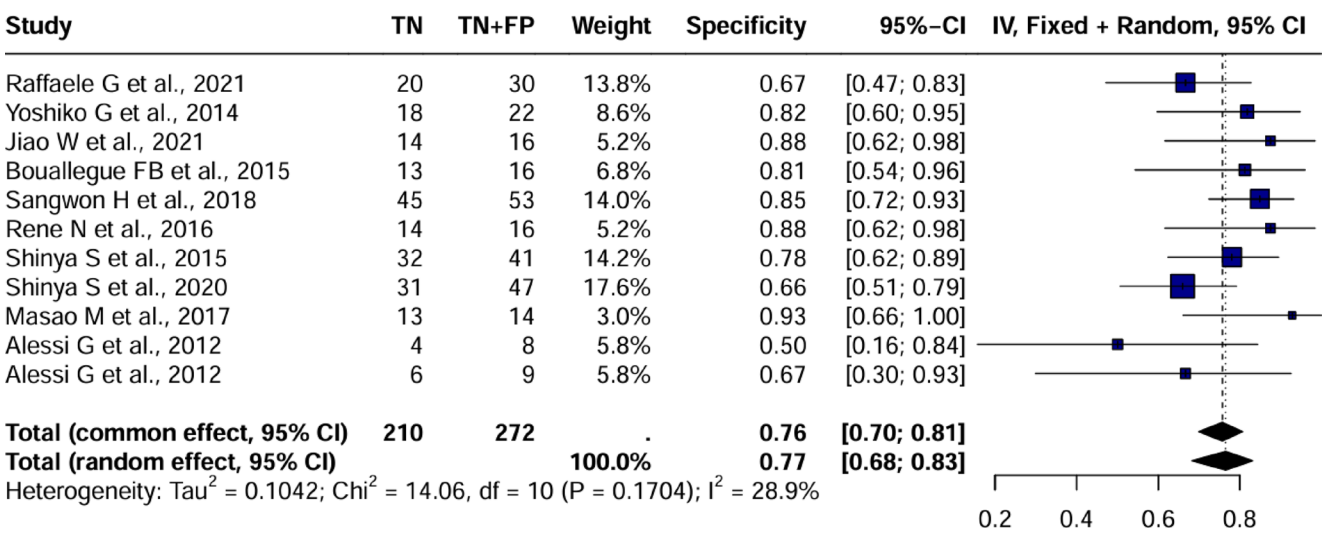

Fig. 3 Forest Plot for Specificity

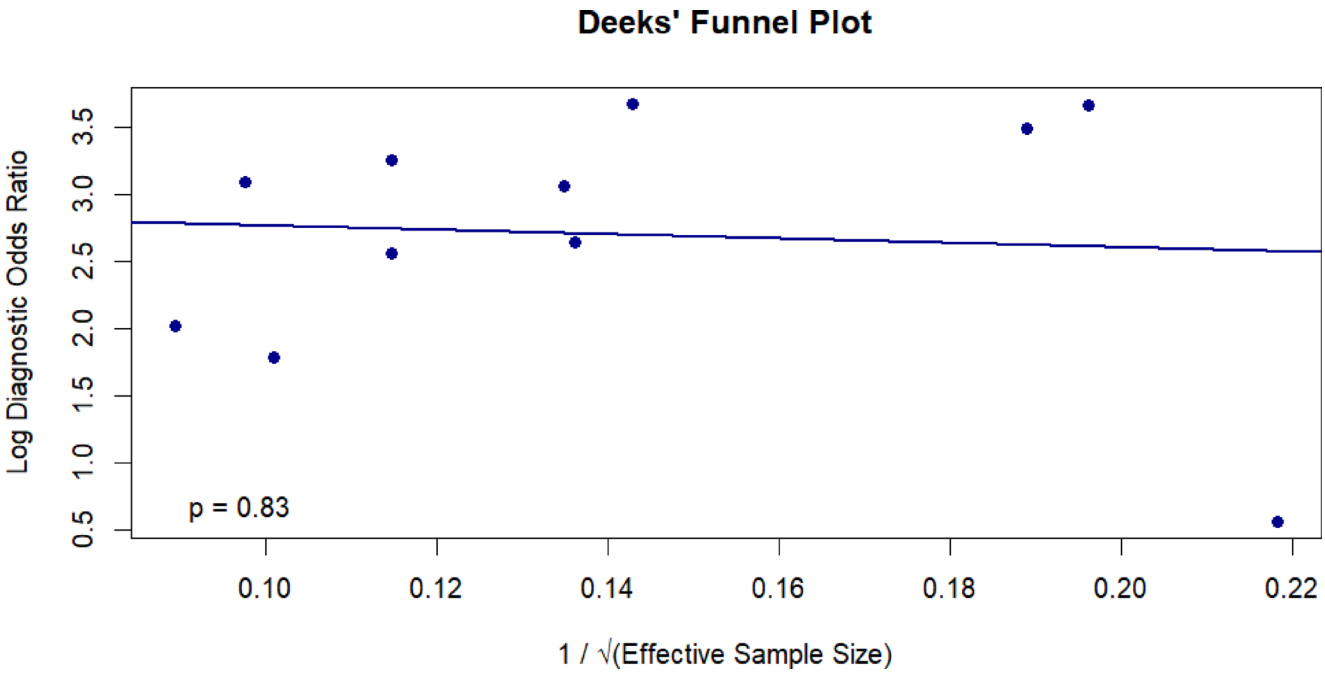

Fig. 4 Assessment of Publication Bias

expensive and, under certain conditions, exhibit more specific targeting abilities for biologically active molecules due to their longer half-lives, which can range from a few hours to several days [36]. The limited utility of PET in the USA is also evident from 2022 data, where Medicare billed for 212,106 PET scans, while SPECT was billed six times more frequently, with 1,343,519 scans. This significant disparity highlights the limited utilization of PET scans compared to other imaging modalities for CAD assessment [37].

Our results align with the ESC 2024 guidelines, which recommend myocardial perfusion SPECT for patients with suspected chronic coronary syndrome (CCS) and a moderate to high pre-test likelihood of CAD (15–85%) [38]. The strong diagnostic performance of CZT SPECT confirms its value as a non-invasive and widely accessible alternative to PET, especially in settings where PET is not available. PET-CT is preferred in specific populations, such as obese, younger patients, or those with multivessel disease or microvascular dysfunction [39]. CZT SPECT demonstrates excellent accuracy and practical utility in broader clinical practice. According to the ACC/AHA 2021 Chest Pain Guidelines, PET is preferred over SPECT for diagnosing suspected CAD due to its higher diagnostic performance.

However, the guidelines also acknowledge the limited availability of PET as a significant constraint [40].

The clinical implications of our study are substantial, as these findings not only enhance the diagnostic accuracy of CZT SPECT but also provide benefits that can improve patient compliance and streamline the clinical workflow, ultimately enhancing the overall patient experience. From a research perspective, our results suggest that further studies are needed to investigate the application of CZT SPECT in various clinical settings and its integration with other imaging modalities in CAD diagnosis and management.

Conclusion

In conclusion, our meta-analysis establishes the Discovery NM 530c CZT SPECT as a reliable and clinically effective non-invasive modality for the detection of coronary artery disease (CAD), demonstrating a pooled sensitivity of 0.835 (95% CI: 0.773–0.883) and specificity of 0.758 (95% CI: 0.678–0.823). The diagnostic odds ratio of 15.9 (95% CI: 7.8–24.0) and an AUC of 0.858 indicate excellent discriminatory capacity. Although current guidelines do not distinguish between conventional and CZT-based systems, accumulating evidence suggests that CZT SPECT offers superior accuracy without the need for CT-based attenuation correction. These characteristics support its utility for ruling in and out CAD, potentially reducing reliance on invasive angiography. Future research should emphasize prospective validation in diverse clinical settings, direct comparisons with other modalities, and cost-effectiveness analyses to inform guideline-directed implementation.

Supplementary Information The online version contains supplementary material available at https://doi.org/10.1007/s10554-025-03475-x.

Author contributions Authors' Contributions: Conceptualization: Mohammad Hamza Bin Abdul Malik, Muhammad ArhamMethodology: Mohammad Hamza Bin Abdul Malik, Anfal Hamza, Allah DadFormal analysis and investigation: Muhammad Arham, Muhammad Awais Bin Abdul Malik, Faseeh haiderWriting– original draft preparation: Mohammad Hamza Bin Abdul Malik, Mishal Khan, Talha Sajjad, Muhammad Hammad Arif, Faseeh Haider, Muhammad Ahmad Qureshi-Writing– review and editing: Muhammad Arham, Ali Bin Abdul Jabbar, Muhammad Abdullah, Faseeh HaiderResources: Mohammad Hamza Bin Abdul MalikSupervision: Muhammad Arham, Mohammad Hamza Bin Abdul MalikFinal changes: Muhammad Arham, Faseeh haider, Allah Dad, Kinza Bakht.

Funding None.

Data availability No datasets were generated or analysed during the current study.

Declarations

Competing interests The authors declare no competing interests.

References

1. ASNC imaging guidelines for SPECT nuclear cardiology procedures Stress, protocols, and tracers. J Nucl Cardiol [Internet]. 2016 Jun 1 [cited 2025 Apr 24];23(3):606–39. Available from: https://www.sciencedirect.com/science/article/pii/S1071358123068599
2. Single Photon Emission Computed Tomography (SPECT) Myocardial Perfusion Imaging Guidelines: Instrumentation, Acquisition, Processing, and Interpretation. J Nucl Cardiol [Internet]. 2018 Oct 1 [cited 2025 Apr 24];25(5):1784–846. Available from: https://www.sciencedirect.com/science/article/pii/S1071358123024182
3. Patel MR, Peterson ED, Dai D, Brennan JM, Redberg RF, Anderson HV et al Low Diagnostic Yield of Elective Coronary Angiography. N Engl J Med [Internet]. 2010 Mar 11 [cited 2025 Apr 24];362(10):886–95. Available from: https://www.nejm.org/doi/full/https://doi.org/10.1056/NEJMoa0907272
4. Curzen N, Nicholas Z, Stuart B, Wilding S, Hill K, Shambrook J et al (2021) Fractional flow reserve derived from computed tomography coronary angiography in the assessment and management of stable chest pain: the FORECAST randomized trial. Eur Heart J [Internet]. Oct 1 [cited 2025 Apr 24];42(37):3844–52. Available from: https://doi.org/10.1093/eurheartj/ehab444
5. Diagnostic accuracy of rest/ stress ECG-gated Rb-82 myocardial perfusion PET: Comparison with ECG-gated Tc-99m sestamibi SPECT. J Nucl Cardiol [Internet]. 2006 Jan 1 [cited 2025 Apr 24];13(1):24–33. Available from: https://www.sciencedirect.com/science/article/abs/pii/S1071358105005878
6. https://www.asnc.org/ [Internet]. [cited 2025 Apr 24]. Clinical quantification of myocardial blood flow using PET: Joint Position Paper of the SNMMI Cardiovascular Council and the ASNC–ASNC. Available from: https://www.asnc.org/resource/clinical-quantification-of-myocardial-blood-flow-using-pet-joint-position-paper-of-the-snmmi-cardiovascular-council-and-the-asnc/
7. New Cardiac Cameras: Single-Photon Emission CT and PET. Semin Nucl Med [Internet] (2014) Jul 1 [cited 2025 Apr 24];44(4):232–51. Available from: https://www.sciencedirect.com/science/article/abs/pii/S0001299814000233
8. Dorbala S, Ando Y, Bokhari S, Dispenzieri A, Falk RH, Ferrari VA et al ASNC/AHA/ASE/EANM/HFSA/ISA/SCMR/SNMMI Expert Consensus Recommendations for Multimodality Imaging in Cardiac Amyloidosis: Part 1 of 2—Evidence Base and Standardized Methods of Imaging. Circ Cardiovasc Imaging [Internet]. 2021 Jul [cited 2025 Apr 24];14(7):e000029. Available from: https://www.ahajournals.org/doi/https://doi.org/10.1161/HCI.0000000000000029
9. Multi-center study of inter-rater reproducibility, image quality, and diagnostic accuracy of CZT versus conventional SPECT myocardial perfusion imaging. J Nucl Cardiol [Internet]. 2023 Apr 1 [cited 2025 Apr 25];30(2):528–39. Available from: https://www.sciencedirect.com/science/article/pii/S1071358123001538
10. Panjer M, Dobrolinska M, Wagenaar NRL, Slart RHJA Diagnostic accuracy of dynamic CZT-SPECT in coronary artery disease. A systematic review and meta-analysis. J Nucl Cardiol [Internet]. 2022 [cited 2025 Apr 25];29(4):1686–97. Available from: https://www.ncbi.nlm.nih.gov/pmc/articles/PMC9345813/
11. Advances in SPECT and PET Hardware. Prog Cardiovasc Dis [Internet] (2015) May 1 [cited 2025 Apr 25];57(6):566–78.

Available from: https://www.sciencedirect.com/science/article/abs/pii/S0033062015000110
12. PRISMA statement [Internet] [cited 2025 Apr 25]. DTA. Available from: https://www.prisma-statement.org/dta
13. Reitsma JB, Glas AS, Rutjes AWS, Scholten RJPM, Bossuyt PM, Zwinderman AH Bivariate analysis of sensitivity and specificity produces informative summary measures in diagnostic reviews. J Clin Epidemiol [Internet]. 2005 Oct 1 [cited 2025 Apr 25];58(10):982–90. Available from: https://www.jclinepi.com/article/S0895-4356(05)00162-9/abstract
14. West RM Best practice in statistics: The use of log transformation. Ann Clin Biochem [Internet]. 2022 May [cited 2025 Apr 25];59(3):162–5. Available from: https://www.ncbi.nlm.nih.gov/pmc/articles/PMC9036143/
15. Seiffert S, Weber S, Sack U, Keller T Use of logit transformation within statistical analyses of experimental results obtained as proportions: example of method validation experiments and EQA in flow cytometry. Front Mol Biosci [Internet]. 2024 Jul 11 [cited 2025 Apr 25];11. Available from: https://www.frontiersin.orghttps://www.frontiersin.org/journals/molecular-biosciences/articles/https://doi.org/10.3389/fmolb.2024.1335174/full
16. Higgins JPT, Green S (editors). Cochrane Handbook for Systematic Reviews of Interventions Version 5.1.0 [updated March 2011]. The Cochrane Collaboration, 2011 https://www.cochrane.org/handbook
17. Cerullo E, Sutton AJ, Jones HE, Wu O, Quinn TJ, Cooper NJ MetaBayesDTA: codeless Bayesian meta-analysis of test accuracy, with or without a gold standard. BMC Med Res Methodol [Internet]. 2023 May 25 [cited 2025 Apr 25];23:127. Available from: https://www.ncbi.nlm.nih.gov/pmc/articles/PMC10210277/
18. A review of solutions for diagnostic accuracy studies with an imperfect or missing reference standard. J Clin Epidemiol [Internet]. 2009 Aug 1 [cited 2025 Apr 25];62(8):797–806. Available from: https://www.sciencedirect.com/science/article/abs/pii/S0895435609000638
19. New measures improved the reporting of heterogeneity in diagnostic test accuracy reviews: a metaepidemiological study. J Clin Epidemiol [Internet]. 2021 Mar 1 [cited 2025 Apr 25];131:101–12. Available from: https://www.sciencedirect.com/science/article/abs/pii/S089543562031180X
20. White SJ, Phua QS, Lu L, Yaxley KL, McInnes MDF, To MS Heterogeneity in Systematic Reviews of Medical Imaging Diagnostic Test Accuracy Studies. JAMA Netw Open [Internet]. 2024 Feb 29 [cited 2025 Apr 25];7(2):e240649. Available from: https://www.ncbi.nlm.nih.gov/pmc/articles/PMC10905313/
21. Lee YH (2015) Meta-Analysis of Diagnostic Test Accuracy. Hanyang Med Rev [Internet]. Feb 26 [cited 2025 Apr 25];35(1):50–3. Available from: https://synapse.koreamed.org/articles/1044250
22. Deeks JJ, Macaskill P, Irwig L (2005) The performance of tests of publication bias and other sample size effects in systematic reviews of diagnostic test accuracy was assessed. Journal of Clinical Epidemiology. 58(9):882–93. https://doi.org/10.1016/j.jclinepi.2005.01.016
23. Xu J, Cai F, Geng C, Wang Z, Tang X (2021) Diagnostic Performance of CMR, SPECT, and PET Imaging for the Identification of Coronary Artery Disease: A Meta-Analysis. Front Cardiovasc Med [Internet]. May 7 [cited 2025 Apr 25];8:621389. Available from: https://www.ncbi.nlm.nih.gov/pmc/articles/PMC8138058/
24. Acampa W, Zampella E, Assante R, Genova A, De Simini G, Mannarino T et al (2021) Quantification of myocardial perfusion reserve by CZT-SPECT: A head to head comparison with 82Rubidium PET imaging. J Nucl Cardiol Off Publ Am Soc Nucl Cardiol 28(6):2827–2839
25. Virani SS, Newby LK, Arnold SV, Bittner V, Brewer LC, Demeter SH, AHA/ACC/ACCP/, ASPC/NLA/PCNA Guideline for the Management of Patients With Chronic Coronary Disease. JACC [Internet] (2023) 2023 Aug 29 [cited 2025 Apr 25];82(9):833–955. Available from: https://www.jacc.org/doi/https://doi.org/10.1016/j.jacc.2023.04.003
26. Kalantari F, Mohseninia N, Wetsch A, Harsini S, Hehenwarter L, Schweighofer-Zwink G et al Head-to-Head Comparison of CZT-SPECT and SPECT/CT Myocardial Perfusion Imaging: Interobserver and Intraobserver Agreement and Diagnostic Performance. Life [Internet]. 2023 Sep 7 [cited 2025 Apr 25];13(9):1879. Available from: https://www.ncbi.nlm.nih.gov/pmc/articles/PMC10532584/
27. Vardhan M, Tanade C, Chen SJ, Mahmood O, Chakravartti J, Jones WS et al (2024) Diagnostic performance of coronary angiography derived computational fractional flow reserve. J Am Heart Assoc 13(13):e029941
28. Koo BK, Erglis A, Doh JH, Daniels DV, Jegere S, Kim HS et al (2011) Diagnosis of ischemia-causing coronary stenoses by noninvasive fractional flow reserve computed from coronary computed tomographic angiograms. J Am Coll Cardiol 58(19):1989–1997
29. Coenen A, Lubbers MM, Kurata A, Kono A, Dedic A, Chelu RG et al (2015) Fractional flow reserve computed from noninvasive CT angiography data: diagnostic performance of an on-site clinician-operated computational fluid dynamics algorithm. Radiology 274(3):674–683
30. Mickley H, Veien KT, Gerke O, Lambrechtsen J, Rohold A, Steffensen FH et al (2022) Diagnostic and clinical value of FFRCT in stable chest pain patients with extensive coronary calcification: the FACC study. JACC Cardiovasc Imaging 15(6):1046–1058
31. The current status of CZT SPECT myocardial blood flow and reserve assessment Tips and tricks. J Nucl Cardiol [Internet]. 2022 Dec 1 [cited 2025 Apr 25];29(6):3137–51. Available from: https://www.sciencedirect.com/science/article/abs/pii/S1071358123006311
32. Diagnostic Performance of Noninvasive Myocardial Perfusion Imaging Using Single-Photon Emission Computed Tomography, Cardiac Magnetic Resonance, and Positron Emission Tomography Imaging for the Detection of Obstructive Coronary Artery Disease: A Meta-Analysis. J Am Coll Cardiol [Internet] (2012) May 8 [cited 2025 Apr 25];59(19):1719–28. Available from: https://www.sciencedirect.com/science/article/pii/S0735109712007000
33. Diagnostic Accuracy of Cardiac Positron Emission Tomography Versus Single Photon Emission Computed Tomography for Coronary Artery Disease [Internet]. [cited 2025 Apr 25]. Available from: https://www.ahajournals.org/doi/epub/https://doi.org/10.1161/CIRCIMAGING.112.978270
34. Prognostic value of myocardial perfusion imaging by cadmium zinc telluride single-photon emission computed tomography in patients with suspected or known coronary artery disease: a systematic review and meta-analysis| European Journal of Nuclear Medicine and Molecular Imaging [Internet]. [cited 2025 Apr 25]. Available from: https://link.springer.com/article/https://doi.org/10.1007/s00259-023-06344-8#Sec16
35. Hlatky MA, Shilane D, Hachamovitch R, Dicarli MF, Investigators SPARC (2014) Economic outcomes in the study of myocardial perfusion and coronary anatomy imaging roles in coronary artery disease registry: the SPARC study. J Am Coll Cardiol 63(10):1002–1008
36. Crișan G, Moldovean-Cioroianu NS, Timaru DG, Andrieș G, Căinap C, Chiș V Radiopharmaceuticals for PET and SPECT Imaging: A Literature Review over the Last Decade. Int J Mol Sci [Internet]. 2022 Apr 30 [cited 2025 Apr 25];23(9):5023. Available from: https://www.ncbi.nlm.nih.gov/pmc/articles/PMC9103893/
37. Cardiac positron emission tomography and other modalities for coronary artery disease assessment: A snapshot from the medicare data. J Nucl Cardiol [Internet]. 2024 Nov 1 [cited 2025 Apr

25];41:102030. Available from: https://www.sciencedirect.com/science/article/abs/pii/S1071358124007128
38. Vrints C, Andreotti F, Koskinas KC, Rossello X, Adamo M, Ainslie J et al 2024 ESC Guidelines for the management of chronic coronary syndromes: Developed by the task force for the management of chronic coronary syndromes of the European Society of Cardiology (ESC) Endorsed by the European Association for Cardio-Thoracic Surgery (EACTS). Eur Heart J [Internet]. 2024 Sep 21 [cited 2025 Apr 25];45(36):3415–537. Available from: https://doi.org/10.1093/eurheartj/ehae177
39. Groepenhoff F, Klaassen RGM, Valstar GB, Bots SH, Onland-Moret NC, Den Ruijter HM et al (2021) Evaluation of non-invasive imaging parameters in coronary microvascular disease: a systematic review. BMC Med Imaging 21(1):5
40. American College of Cardiology [Internet] [cited 2025 Apr 25]. Key Imaging Takeaways From the 2021 Chest Pain Guidelines. Available from: https://www.acc.org/Latest-in-Cardiology/Articles/2022/03/14/11/34/http%3a%2f%2fwww.acc.org%2fLatest-in-Cardiology%2fArticles%2f2022%2f03%2f14%2f11%2f34%2fKey-Imaging-Takeaways-From-the-2021-Chest-Pain-Guidelines

Authors and Affiliations

Muhammad Arham[1] · Allah Dad[1] · Mohammad Hamza Bin Abdul Malik[2] · Talha Sajjad[1] · Muhammad Awais Bin[1] · Faseeh Haider[3] · Mishal Khan[4] · Anfal Hamza[1] · Muhammad Hammad Arif[5] · Muhammad Ahmad Qureshi[6] · Ali Bin Abdul Jabbar[7] · Muhammad Abdullah Javed[8] · Kinza Bakht[1]

✉ Faseeh Haider
faseehhaidermd@gmail.com

Muhammad Arham
md.muhammadarham@gmail.com

Allah Dad
4mbbs928@gmail.com

Mohammad Hamza Bin Abdul Malik
m.hamzabinmalik@gmail.com

Talha Sajjad
md.talha.sajjad@gmail.com

Muhammad Awais Bin
awaisbinmalik@gmail.com

Mishal Khan
mishalkk17@gmail.com

Anfal Hamza
anfalhamza432@gmail.com

Muhammad Hammad Arif
hammad.arif202@gmail.com

Muhammad Ahmad Qureshi
ahmadqur267@gmail.com

Ali Bin Abdul Jabbar
alibinabduljabbar@creighton.edu

Muhammad Abdullah Javed
muhammadabdullah.javed@bcm.edu

Kinza Bakht
Kinzabakht02@gmail.com

1 Sheikh Zayed Medical College/Hospital, Rahim Yar Khan, Pakistan

2 Nassau University Medical Center, New York, US

3 Department of medicine, Allama Iqbal Medical college, Lahore, Pakistan

4 Pakistan Institute of Medical Sciences, Islamabad, Pakistan

5 D.G Khan Medical College, Dera Ghazi Khan, Pakistan

6 Henry Ford Jackson Hospital, New york, US

7 Department of Medicine, Creighton University School of Medicine, Omaha, NE, US

8 Department of Medicine, Baylor College of Medicine, Houston, TX, US